Scientific
Research

Li₂MnSiO₄/Carbon Composite Nanofibers as a High-Capacity Cathode Material for Li-Ion Batteries

Shu Zhang, Ying Li, Guanjie Xu, Shuli Li, Yao Lu, Ozan Topracki, Xiangwu Zhang*

Fiber and Polymer Science Program, Department of Textile Engineering, Chemistry and Science, North Carolina State University, Raleigh, USA.
Email: *xiangwu_zhang@ncsu.edu

ABSTRACT

Li₂MnSiO₄ has an extremely high theoretical capacity of 332 mAh·g⁻¹. However, only around half of this capacity has been realized in practice and the capacity retention during cycling is also low. In this study, Li₂MnSiO₄/carbon composite nanofibers were prepared by a combination of electrospinning and heat treatment. The one-dimensional continuous carbon nanofiber matrix serves as long-distance conductive pathways for both electrons and ions. The composite nanofiber structure avoids the aggregation of Li₂MnSiO₄ particles, which in turn enhances the electrode conductivity and promotes the reaction kinetics. The resultant Li₂MnSiO₄/carbon composite nanofibers were used as the cathode material for Li-ion batteries, and they delivered high charge and discharge capacities of 218 and 185 mAh·g⁻¹, respectively, at the second cycle. In addition, the capacity retention of Li₂MnSiO₄ at the first 20th cycles increased from 37% to 54% in composite nanofibers.

Keywords: Electrospinning; Li₂MnSiO₄; Carbon Nanofibers; Li-Ion Battery

1. Introduction

The expanding demand for large-scale commercialization of Li-ion batteries with high energy and power densities has motivated active research on electrode materials with higher capacity and better performance. Goodenough's [1] discovery of LiFePO₄ as cathode materials has changed the landscape of Li-ion batteries due to its high stability and reliable safety. However, LiFePO₄ can only provide one lithium ion per formula unit, and hence its theoretical capacity is only 167 mAh·g⁻¹ [2,3]. Nyten [4,5] firstly synthesized and characterized Li₂FeSiO₄, which not only has the same benefits as LiFePO₄, but also can theoretically extract two lithium ions per formula unit from the structure. The extraction of two lithium ions leads to a high theoretical capacity of 320 mAh·g⁻¹ for Li₂FeSiO₄. However, electrochemical tests only realized less than one lithium extraction per transitional metal in practice (*i.e.*, <160 mAh·g⁻¹) [4,5]. Dominko [6] then proposed the substitution of Fe with Mn. It was anticipated that with two redox pairs of Mn(II)/Mn(III) and Mn(III)/Mn(IV), the two-electron reaction could become possible, corresponding to a high theoretical capacity of 332 mAh·g⁻¹. However, they only achieved 0.7 lithium ion per formula unit during charge/discharge, and serious capacity loss was also observed during cycling. The poor conductivity

and slow kinetics for Li₂FeSiO₄ and Li₂MnSiO₄ is probably the main reason why researchers have not been able to extract reversibly more than one lithium ion per formula unit for these cathode materials [4-6].

Extensive research on many cathode materials suggested that size reduction and conducting phase embedding could overcome the kinetic problem. We herein report a novel approach to prepare Li₂MnSiO₄/carbon nanofibers by electrospinning and heat treatment. During electrospinning, the synthesized Li₂MnSiO₄ particles were embedded into polymer nanofibers. The heat treatment step converted the polymer into a conductive carbon nanofiber matrix to provide enhanced electron and ion diffusions. The prepared Li₂MnSiO₄/carbon nanofibers show improved capacity and reversibility.

2. Experimental

2.1. Material Preparation

The starting materials for Li₂MnSiO₄ were lithium acetate dihydrate (98%, powder, Acros Organics), manganese (II) acetate (98%, powder, Sigma-Aldrich), and SiO₂ nanoparticles (Aerosil 90, Riedel-del Haen) with a molar ratio of 2:1:1. Ethylene glycol (Sigma-Aldrich) and citric acid (Sigma-Aldrich) were also added as complexant for SiO₂ in a molar ratio of 1:2:1 with regard to

---

*Corresponding author.

the amount of SiO$_2$ added. The mixture was subjected to vigorous magnetic stirring, followed by drying in a vacuum oven at 80°C for 24 hr. Dried mixture was ground and calcined in a furnace (Lucifer furnaces, Inc.) at 700°C for 12 hr with a constant flow of argon gas. The obtained sample was ground into fine Li$_2$MnSiO$_4$ powder with mortar and pestle for an hour.

An 8 wt% polyacrylonitrile (PAN, Mw = 150,000, powder, Pfaultz & Bauer Inc.) solution in dimethylformamide (DMF, Sigma-Aldrich) was prepared at 60°C. A homogeneously distributed dispersion was obtained by adding 30 wt% Li$_2$MnSiO$_4$ into the PAN solution, following by mechanical stirring overnight. The dispersion was drawn into a syringe, which was secured in a syringe pump with a flow rate of 1 mL·hr^{-1}. The electrospinning of nanofibers was carried out with a voltage of 18 kV and a needle tip-to-collector distance of 15 cm. The electrospun Li$_2$MnSiO$_4$/PAN composite nanofibers were first heated and stabilized at 280°C under air atmosphere for 5 hrs with a heating rate of 5°C·min^{-1}, following by raising the temperature to 700°C with a heating rate of 2°C·min^{-1} under argon. To complete the carbonization procedure, the nanofibers composite was held at the final temperature under a constant argon flow for 8 hr. The resultant Li$_2$MnSiO$_4$/carbon composite nanofibers were then used as the cathode material for Li-ion batteries.

2.2. Structure Characterization

The morphology and diameter of both Li$_2$MnSiO$_4$ powder and Li$_2$MnSiO$_4$/carbon composite nanofibers were evaluated by scanning electron microscope (SEM, JEOL 6400F FESEM) and field emission electron microscope (FETEM, Hitachi HF2000). X-ray diffraction (Rigaku SmartLab) was performed to identify the structural variations.

2.3. Performance Evaluation

The electrochemical performance was investigated using two-electrode coin-type half cells. For the Li$_2$MnSiO$_4$ powder, the electrode was assembled by coating the slurry of 80 wt% active material, 10 wt% conductive carbon black, and 10 wt% polyvinylidene fluoride (PVdF) in N-methylpyrrolidinone (NMP) on an aluminum foil of 0.5 inch in diameter. For Li$_2$MnSiO$_4$/carbon composite nanofibers, they formed free-standing and flexible mats and were directly cut into binder-free electrodes with a diameter of 1/2 inch. Li sheet was used as the counter electrode, and polypropylene (PP) film (Celgard 2400) as the separator. The electrolyte used was purchased from MTI corporation with 1 M solution of LiPF$_6$ in a mixture (1:1:1 by volume) of ethylene carbonate (EC), dimethyl carbonate (DMC) and diethyl carbonate (DEC). The galvanostatic charge/discharge characteristics of the cells

were recorded with a LAND battery testing system in the voltage range of 2.0 - 5.0 V (versus Li/Li$^+$) at room temperature.

3. Results and Discussion

3.1. Nanofiber Structure

Figure 1 shows SEM images of the Li$_2$MnSiO$_4$ powder. The synthesized Li$_2$MnSiO$_4$ powder consists of agglomerated nanoparticles with primary particle size in the range of 30 - 50 nm.

Figures 2(A)-(C) show SEM images of Li$_2$MnSiO$_4$/PAN precursor nanofibers. Electrospun Li$_2$MnSiO$_4$/PAN nanofibers exhibit a rough fiber surface due to the presence of Li$_2$MnSiO$_4$ particles. The diameter of Li$_2$MnSiO$_4$/PAN nanofibers is in the range of 250 - 360 nm. SEM images of Li$_2$MnSiO$_4$/carbon composite nanofibers are presented in **Figures 2(D)** and **(E)**. After heat treatment, substantial volume contraction and fiber diameter reduction were observed due to the removal of some species during the heat treatment process. The diameter of Li$_2$MnSiO$_4$/carbon nanofibers is in the range of 180 - 280 nm. **Figure 3** shows a TEM image of a Li$_2$MnSiO$_4$/carbon composite nanofiber. It is seen that the Li$_2$MnSiO$_4$ particles are dispersed in the carbon nanofiber matrix, which can provide excellent electronic conduction.
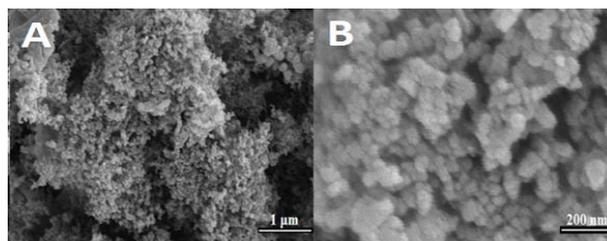
Figure 1. SEM images of Li$_2$MnSiO$_4$ particle at different magnifications.
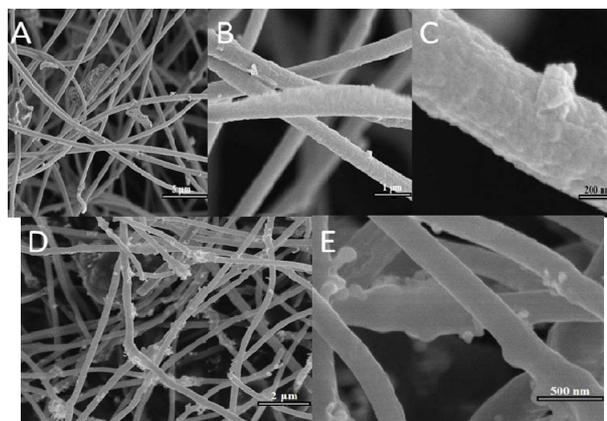
Figure 2. SEM images of electrospun Li$_2$MnSiO$_4$/PAN nanofibers (A, B, and C) and Li$_2$MnSiO$_4$/carbon nanofibers (D and E) at different magnifications.
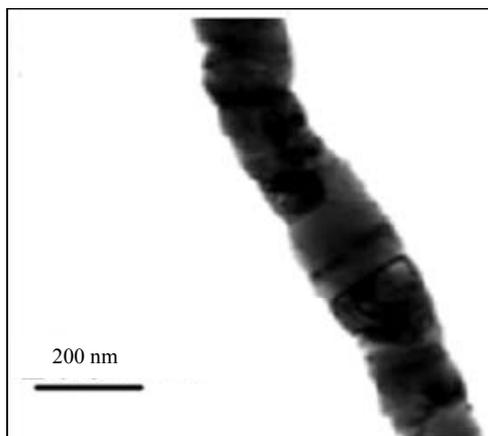
Figure 3. TEM image of a Li$_2$MnSiO$_4$/carbon composite nanofiber.

The XRD patterns of Li$_2$MnSiO$_4$ powder and Li$_2$Mn-SiO$_4$/carbon nanofibers are shown in **Figure 4**. It is seen that in both Li$_2$MnSiO$_4$ powder and Li$_2$MnSiO$_4$/carbon nanofibers, Li$_2$MnSiO$_4$ exists in the form of a stoichiometric orthorhombic structure with Pmn2$_1$ space group [7]. The signal of MnO was also detected at around $2\theta =$ 41° for both samples, which is considered as an impurity for Li$_2$MnSiO$_4$. The XRD pattern of Li$_2$MnSiO$_4$/carbon nanofibers appears to be identical to that of Li$_2$MnSiO$_4$ powder, indicating that the heat treatment did not change the structure of the active material.

3.2. Nanofiber Performance

Figure 5 shows representative charge-discharge curves of both Li$_2$MnSiO$_4$ powder and Li$_2$MnSiO$_4$/carbon composite nanofibers. The cells were cycled at a current density of C/20 between 2.0 and 5.0 V. At the second cycle, the charge and discharge capacities of Li$_2$MnSiO$_4$ powder are 215 and 176 mAh·g^{-1}, respectively. Incorporating Li$_2$MnSiO$_4$ into composite carbon nanofibers increases the second-cycle charge and discharge capacities to 218 and 185 mAh·g^{-1}, respectively. The reversible capacity for one electron transfer per transition metal is 167 mAh·g^{-1}. Therefore, an electrochemical reaction of more than one electron transfer has been realized.

From **Figure 5**, it is also seen that Li$_2$MnSiO$_4$ powder has a discharge capacity of only 80 mAh·g^{-1} after 20 cycles, corresponding to a capacity retention of 37%. However, Li$_2$MnSiO$_4$/carbon composite nanofibers exhibit a higher capacity retention of 54% at 20th cycle. The electrochemical performance, especially the cycling behavior, is directly related to the robustness of the electrical contact between active particles. Embedding active particles into a carbon nanofiber matrix can lead to higher and more robust electronic conductivity of the electrodes [8,9]. The enhanced cycling performance of Li$_2$MnSiO$_4$/carbon nanofibers may be attributed to the
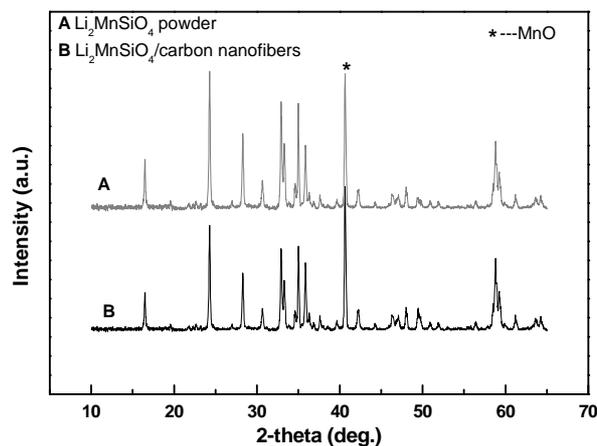
Figure 4. X-ray diffraction patterns of (A) Li$_2$MnSiO$_4$ powder, and (B) Li$_2$MnSiO$_4$/carbon nanofibers.

(a)

(b)
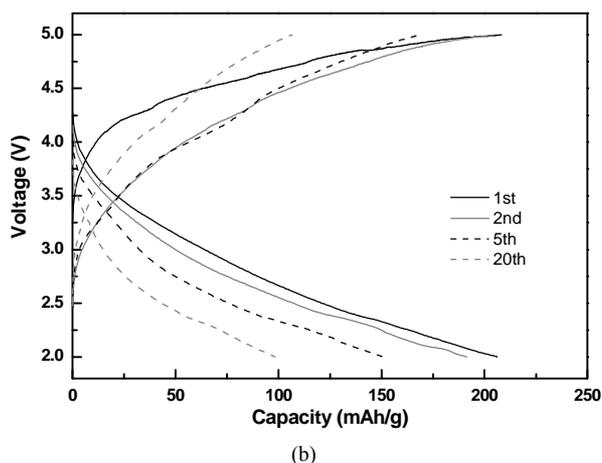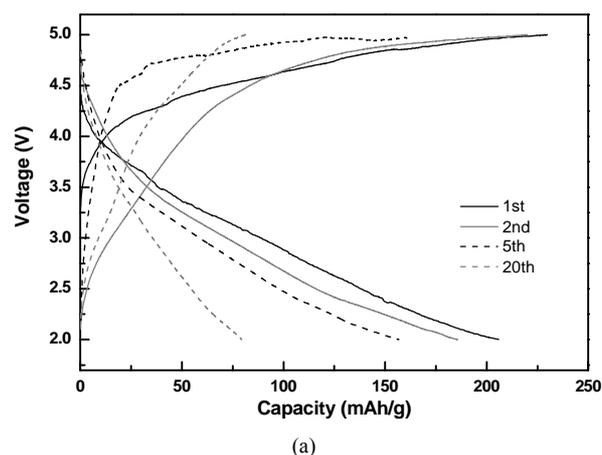
Figure 5. Galvanostatic charge-discharge curves of (a) Li$_2$MnSiO$_4$ powder, and (b) Li$_2$MnSiO$_4$/carbon nanofibers.

improved electronic conductivity provided by the carbon nanofiber matrix with more effective pathways and shorter diffusion lengths for both ions and electrons. In addition to facilitating charge transfer among active particles, the hybridization of carbon nanofibers with active

Li$_2$MnSiO$_4$ particles also keeps the primary Li$_2$MnSiO$_4$ particles from further aggregation by confining them in the nanofibrous network structure [3].

4. Summary

Li$_2$MnSiO$_4$/carbon nanofibers were prepared by electrospinning and heat treatment. For comparison, Li$_2$MnSiO$_4$ powder was also prepared. Li$_2$MnSiO$_4$ powder showed charge and discharge capacities of 215 and 176 mAh·g^{-1}, respectively, at the second cycle. These capacities faded dramatically with a capacity loss of 63% at the 20th cycle. Incorporating Li$_2$MnSiO$_4$ particles into carbon nanofibers resulted in slightly increased charge and discharge capacities of 218 and 185 mAh·g^{-1}, respectively, at the second cycle, indicating an electrochemical reaction of more than one electron transfer per transition metal. In addition, the capacity retention was improved to 54% after 20 cycles.

5. Acknowledgements

REFERENCES

[1] M. M. Thackeray, W. I. F. David, P. G. Bruce and J. B. Goodenough, "Lithium Insertion into Manganese Spinels," *Materials Research Bulletin*, Vol. 18, No. 4, 1983, pp. 461-472. doi:10.1016/0025-5408(83)90138-1

[2] S. Yang, Y. Song, P. Y. Zavalij and M. S. Whittingham, "Reactivity, Stability and Electrochemical Behavior of Lithium Iron Phosphates," *Electrochemistry Communica-tions*, Vol. 4, No. 3, 2002, pp. 239-244.

[3] O. Toprakci, L. Ji, Z. Lin, H. A. K. Toprakci and X. Zhang, "Fabrication and Electrochemical Characteristics of Electrospun LiFePO$_4$/Carbon Composite Fibers for Lithium-Ion Batteries," *Journal of Power Sources*, Vol. 196, No. 18, 2011, pp. 7692-7699. doi:10.1016/j.jpowsour.2011.04.031

[4] A. Nyten, A. Abouimrane, M. Armand, T. Gustafsson and J. O. Thomas, "Elelctrochemical Performance of Li$_2$FeSiO$_4$ as a New Cathode Material," *Materials Chemistry*, Vol. 7, 2005, pp. 156-160.

[5] A. Nyten, S. Kamali, L. Hanggstrom, T. Gustafsson and J. O. Thomas, "The Lithium Extraction/Insertion Mechanism in Li$_2$FeSiO$_4$," *Materials Chemistry*, Vol. 16, 2006, pp. 2266-2272. doi:10.1039/b601184e

[6] R. Dominko, M. Bele, A. Kokalj, M. Gaberscek and J. Jamnik, "Li$_2$MnSiO$_4$ as a Potential Li-Battery Cathode Material," *Journal of Power Sources*, Vol. 174, No. 2, 2007, pp. 457-461. doi:10.1016/j.jpowsour.2007.06.188

[7] R. Dominko, M. Bele, M. Gaberscek, A. Meden, M. Remskar and J. Jamnik, "Structure and Electrochemical Performance of Li$_2$MnSiO$_4$ and Li$_2$FeSiO$_4$ as Potential Li-Battery Cathode Materials," *Electrochemistry Communications*, Vol. 8, No. 2, 2006, pp. 217-222. doi:10.1016/j.elecom.2005.11.010

[8] Z. Lin, L. Ji, M. Woodroof and X. Zhang, "Electrodeposited MnO$_x$/Carbon Nanofiber Composites for Use as Anode Materials in Rechargeable Lithium-Ion Batteries," *Journal of Power Sources*, Vol. 195, No. 15, 2010, pp. 5025-5031. doi:10.1016/j.jpowsour.2010.02.004

[9] L. Ji, Z. Lin, A. J. Medford and X. Zhang, "*In-Situ* Encapsulation of Nickel Particles in Electrospun Carbon Nanofibers and Their Electrochemical Performance," *Chemistry—A European Journal*, Vol. 15, No. 41, 2009, pp. 10718-10722. doi:10.1002/chem.200902012